

Time-Dependent CP Asymmetries in $B^0 \rightarrow K_S^0 \pi^0$ transitions

K.Abe,⁹ K.Abe,⁴⁹ I.Adachi,⁹ H.Aihara,⁵¹ D.Anipko,¹ K.Aoki,²⁵ T.Arakawa,³²
 K.Arinstein,¹ Y.Asano,⁵⁶ T.Aso,⁵⁵ V.Aulchenko,¹ T.Aushev,²¹ T.Aziz,⁴⁷ S.Bahinipati,⁴
 A.M.Bakich,⁴⁶ V.Balagura,¹⁵ Y.Ban,³⁷ S.Banerjee,⁴⁷ E.Barberio,²⁴ M.Barbero,⁸
 A.Bay,²¹ I.Bedny,¹ K.Bebus,¹⁴ U.Bitenc,¹⁶ I.Bizjak,¹⁶ S.Blyth,²⁷ A.Bondar,¹
 A.Bozek,³⁰ M.Bracko,^{23,16} J.Brodzicka,^{9,30} T.E.Browder,⁸ M.-C.Chang,⁵⁰ P.Chang,²⁹
 Y.Chao,²⁹ A.Chen,²⁷ K.-F.Chen,²⁹ W.T.Chen,²⁷ B.G.Cheon,³ R.Chistov,¹⁵
 J.H.Choi,¹⁸ S.K.Choi,⁷ Y.Choi,⁴⁵ Y.K.Choi,⁴⁵ A.Chuvikov,³⁹ S.Cole,⁴⁶ J.Dalseno,²⁴
 M.Danilov,¹⁵ M.Dash,⁵⁷ R.Dowd,²⁴ J.Dragic,⁹ A.Dnutskey,⁴ S.Eidelman,¹ Y.Enari,²⁵
 D.Epifanov,¹ S.Fratina,¹⁶ H.Fujii,⁹ M.Fujikawa,²⁶ N.Gabyshev,¹ A.Gamash,³⁹
 T.Gershon,⁹ A.Go,²⁷ G.Gokhroo,⁴⁷ P.Goldenzweig,⁴ B.Golob,^{22,16} A.Gorisek,¹⁶
 M.Grosse Perdekamp,^{11,40} H.Guler,⁸ H.Ha,¹⁸ J.Haba,⁹ K.Hara,²⁵ T.Hara,³⁵
 Y.Hasegawa,⁴⁴ N.C.Hastings,⁵¹ K.Hayasaka,²⁵ H.Hayashii,²⁶ M.Hazumi,⁹
 D.Heeman,³⁵ T.Higuchi,⁹ L.Hinz,²¹ T.Hokuue,²⁵ Y.Hoshi,⁴⁹ K.Hoshina,⁵⁴ S.Hou,²⁷
 W.-S.Hou,²⁹ Y.B.Hsiung,²⁹ Y.Igarashi,⁹ T.Iijima,²⁵ K.Ikado,²⁵ A.Imoto,²⁶ K.Inami,²⁵
 A.Ishikawa,⁵¹ H.Ishino,⁵² K.Itoh,⁵¹ R.Itoh,⁹ M.Iwabuchi,⁶ M.Iwasaki,⁵¹ Y.Iwasaki,⁹
 C.Jacoby,²¹ M.Jones,⁸ H.Kakuno,⁵¹ J.H.Kang,⁵⁸ J.S.Kang,¹⁸ P.Kapusta,³⁰
 S.U.Kataoka,²⁶ N.Katayama,⁹ H.Kawai,² T.Kawasaki,³² H.R.Khan,⁵² A.Kibayashi,⁵²
 H.Kichimi,⁹ N.Kikuchi,⁵⁰ H.J.Kim,²⁰ H.O.Kim,⁴⁵ J.H.Kim,⁴⁵ S.K.Kim,⁴³
 T.H.Kim,⁵⁸ Y.J.Kim,⁶ K.Kinoshita,⁴ N.Kishimoto,²⁵ S.Korpar,^{23,16} Y.Kozakai,²⁵
 P.Krizan,^{22,16} P.Krokovny,⁹ T.Kubota,²⁵ R.Kulasiri,⁴ R.Kumar,³⁶ C.C.Kuo,²⁷
 E.Kurihara,² A.Kusaka,⁵¹ A.Kuzmin,¹ Y.-J.Kwon,⁵⁸ J.S.Lange,⁵ G.Leder,¹³ J.Lee,⁴³
 S.E.Lee,⁴³ Y.-J.Lee,²⁹ T.Lesiak,³⁰ J.Li,⁸ A.Limosani,⁹ C.Y.Lin,²⁹ S.-W.Lin,²⁹
 Y.Liu,⁶ D.Liventsev,¹⁵ J.MadNaughton,¹³ G.Majumder,⁴⁷ F.Mandl,¹³ D.Marlou,³⁹
 T.Matsumoto,⁵³ A.Matyja,³⁰ S.McOnie,⁴⁶ T.Medvedeva,¹⁵ Y.Mikami,⁵⁰ W.Mitaro,¹³
 K.Miyabayashi,²⁶ H.Miyake,³⁵ H.Miyata,³² Y.Miyazaki,²⁵ R.Mizuk,¹⁵ D.Mohapatra,⁵⁷
 G.R.Moloney,²⁴ T.Mori,⁵² J.Mueller,³⁸ A.Murakami,⁴¹ T.Nagamine,⁵⁰ Y.Nagasaka,¹⁰
 T.Nakagawa,⁵³ Y.Nakahama,⁵¹ I.Nakamura,⁹ E.Nakano,³⁴ M.Nakao,⁹ H.Nakazawa,⁹
 Z.Natkaniec,³⁰ K.Neichi,⁴⁹ S.Nishida,⁹ K.Nishimura,⁸ O.Nitoh,⁵⁴ S.Noguchi,²⁶
 T.Nozaki,⁹ A.Ogawa,⁴⁰ S.Ogawa,⁴⁸ T.Ohshima,²⁵ T.Okabe,²⁵ S.Okuno,¹⁷ S.L.Olsen,⁸
 S.Ono,⁵² W.Ostrowicz,³⁰ H.Ozaki,⁹ P.Pakhlov,¹⁵ G.Pakhlova,¹⁵ H.Palka,³⁰
 C.W.Park,⁴⁵ H.Park,²⁰ K.S.Park,⁴⁵ N.Parslow,⁴⁶ L.S.Peak,⁴⁶ M.Pemicka,¹³
 R.Pestotnik,¹⁶ M.Peters,⁸ L.E.Piilonen,⁵⁷ A.Poluektov,¹ F.J.Ronga,⁹ N.Root,¹
 J.Rorie,⁸ M.Rozanska,³⁰ H.Sahoo,⁸ S.Saitoh,⁹ Y.Sakai,⁹ H.Sakamoto,¹⁹ H.Sakaue,³⁴
 T.R.Sarangi,⁶ N.Sato,²⁵ N.Satoyama,⁴⁴ K.Sayeed,⁴ T.Schietinger,²¹ O.Schneider,²¹
 P.Schonmeyer,⁵⁰ J.Schumann,²⁸ C.Schwanda,¹³ A.J.Schwartz,⁴ R.Seidl,^{11,40} T.Seki,⁵³
 K.Senyo,²⁵ M.E.Sevior,²⁴ M.Shapkin,¹⁴ Y.-T.Shen,²⁹ H.Shibuya,⁴⁸ B.Shwartz,¹
 V.Sidorov,¹ J.B.Singh,³⁶ A.Sokolov,¹⁴ A.Somov,⁴ N.Soni,³⁶ R.Stamen,⁹ S.Stanic,³³
 M.Staric,¹⁶ H.Stoek,⁴⁶ A.Sugiyama,⁴¹ K.Sumisawa,⁹ T.SumiYoshi,⁵³ S.Suzuki,⁴¹
 S.Y.Suzuki,⁹ O.Tajima,⁹ N.Takada,⁴⁴ F.Takasaka,⁹ K.Tamaki,⁹ N.Tamura,³²
 K.Tanabe,⁵¹ M.Tanaka,⁹ G.N.Taylor,²⁴ Y.Teramoto,³⁴ X.C.Tian,³⁷ I.Tikhomirov,¹⁵

K. Trabelsi,⁹ Y. T. Tsai,²⁹ Y. F. Tse,²⁴ T. Tsuboyama,⁹ T. Tsukamoto,⁹ K. Uchida,⁸
 Y. Uchida,⁶ S. Uehara,⁹ T. Uglav,¹⁵ K. Ueno,²⁹ Y. Unno,⁹ S. Uno,⁹ P. Urquijo,²⁴
 Y. Ushiroda,⁹ Y. Usov,¹ G. Vamer,⁸ K. E. Varvell,⁴⁶ S. Villa,²¹ C. C. Wang,²⁹
 C. H. Wang,²⁸ M. -Z. Wang,²⁹ M. Watanabe,³² Y. Watanabe,⁵² J. Wicht,²¹ L. Widhalm,¹³
 J. Wierchczynski,³⁰ E. Won,¹⁸ C. H. Wu,²⁹ Q. L. Xie,¹² B. D. Yabsley,⁴⁶ A. Yamaguchi,⁵⁰
 H. Yamamoto,⁵⁰ S. Yamamoto,⁵³ Y. Yamashita,³¹ M. Yamachi,⁹ Heyoung Yang,⁴³
 S. Yoshino,²⁵ Y. Yuan,¹² Y. Yusa,⁵⁷ S. L. Zang,¹² C. C. Zhang,¹² J. Zhang,⁹
 L. M. Zhang,⁴² Z. P. Zhang,⁴² V. Zhilich,¹ T. Ziegler,³⁹ A. Zupanc,¹⁶ and D. Zuercher²¹

(The Belle Collaboration)

¹Budker Institute of Nuclear Physics, Novosibirsk

²Chiba University, Chiba

³Chonnam National University, Kwangju

⁴University of Cincinnati, Cincinnati, Ohio 45221

⁵University of Frankfurt, Frankfurt

⁶The Graduate University for Advanced Studies, Hayama

⁷Gyeongsang National University, Chinju

⁸University of Hawaii, Honolulu, Hawaii 96822

⁹High Energy Accelerator Research Organization (KEK), Tsukuba

¹⁰Hiroshima Institute of Technology, Hiroshima

¹¹University of Illinois at Urbana-Champaign, Urbana, Illinois 61801

¹²Institute of High Energy Physics,

Chinese Academy of Sciences, Beijing

¹³Institute of High Energy Physics, Vienna

¹⁴Institute of High Energy Physics, Protvino

¹⁵Institute for Theoretical and Experimental Physics, Moscow

¹⁶J. Stefan Institute, Ljubljana

¹⁷Kanagawa University, Yokohama

¹⁸Korea University, Seoul

¹⁹Kyoto University, Kyoto

²⁰Kyungpook National University, Taegu

²¹Swiss Federal Institute of Technology of Lausanne, EPFL, Lausanne

²²University of Ljubljana, Ljubljana

²³University of Maribor, Maribor

²⁴University of Melbourne, Victoria

²⁵Nagoya University, Nagoya

²⁶Nara Women's University, Nara

²⁷National Central University, Chung-li

²⁸National United University, Miao Li

²⁹Department of Physics, National Taiwan University, Taipei

³⁰H. Niewodniczanski Institute of Nuclear Physics, Krakow

³¹Nippon Dental University, Niigata

³²Niigata University, Niigata

³³University of Nova Gorica, Nova Gorica

³⁴Osaka City University, Osaka

³⁵Osaka University, Osaka

³⁶Punjab University, Chandigarh

- ³⁷Peking University, Beijing
- ³⁸University of Pittsburgh, Pittsburgh, Pennsylvania 15260
- ³⁹Princeton University, Princeton, New Jersey 08544
- ⁴⁰RIKEN BNL Research Center, Upton, New York 11973
- ⁴¹Saga University, Saga
- ⁴²University of Science and Technology of China, Hefei
- ⁴³Seoul National University, Seoul
- ⁴⁴Shinshu University, Nagano
- ⁴⁵Sungkyunkwan University, Suwon
- ⁴⁶University of Sydney, Sydney NSW
- ⁴⁷Tata Institute of Fundamental Research, Bombay
- ⁴⁸Toho University, Funabashi
- ⁴⁹Tohoku Gakuin University, Tagajō
- ⁵⁰Tohoku University, Sendai
- ⁵¹Department of Physics, University of Tokyo, Tokyo
- ⁵²Tokyo Institute of Technology, Tokyo
- ⁵³Tokyo Metropolitan University, Tokyo
- ⁵⁴Tokyo University of Agriculture and Technology, Tokyo
- ⁵⁵Toyama National College of Maritime Technology, Toyama
- ⁵⁶University of Tsukuba, Tsukuba
- ⁵⁷Virginia Polytechnic Institute and State University, Blacksburg, Virginia 24061
- ⁵⁸Yonsei University, Seoul
- (Dated: December 29, 2018)

Abstract

We report measurements of CP-violation parameters in $B^0 \rightarrow K_S^0 \pi^0$ transitions based on a data sample that contains $535 \times 10^6 B\bar{B}$ pairs that was collected near the $(4S)$ resonance, with the Belle detector at the KEKB asymmetric energy e^+e^- collider. One neutral B meson is fully reconstructed in the $B^0 \rightarrow K_S^0 \pi^0$ decay channel with $K_S^0 \pi^0$ invariant mass up to $1.8 \text{ GeV} = c^2$. The flavor of the accompanying B meson is identified from its decay products. CP-violation parameters, S and A , are obtained from the asymmetries in the distribution of the proper-time intervals between the two B decays.

We measure S and A in two $K_S^0 \pi^0$ invariant mass regions. For the full range of $K_S^0 \pi^0$ invariant mass up to $1.8 \text{ GeV} = c^2$, we obtain $S_{K_S^0 \pi^0} = 0.10 \pm 0.31(\text{stat}) \pm 0.07(\text{syst})$ and $A_{K_S^0 \pi^0} = 0.20 \pm 0.20(\text{stat}) \pm 0.06(\text{syst})$. Restricting to $K_S^0 \pi^0$ mass around $K^0(892)$ resonance (0.8 to $1.0 \text{ GeV} = c^2$), we obtain $S_{K^0} = 0.32^{+0.36}_{-0.33}(\text{stat}) \pm 0.05(\text{syst})$ and $A_{K^0} = 0.20 \pm 0.24(\text{stat}) \pm 0.05(\text{syst})$.

PACS numbers: 11.30.Er, 13.25.Hw

Physics parameters related to radiative penguin processes such as $b \rightarrow s \gamma$ are sensitive to physics beyond the standard model (SM). In particular, the phenomena of time-dependent CP violation in decays of the type $B^0 \rightarrow f_{CP}$, where f_{CP} is a final state which is CP eigenstate, have drawn much interest in recent theoretical and experimental work [1]–[7]. Within the SM, the photon emitted from a B^0 (\bar{B}^0) meson is dominantly right-handed (left-handed). A flip of photon polarization only takes place at an order of $2m_s/m_b$, where m_s and m_b are the masses of the s and b quarks. Hence, even though we choose a CP eigenstate such as $K_S^0 \rightarrow K_S^0 \pi^0$ as f_{CP} , the SM predicts a small asymmetry [1, 2]. Naively, the same expectation holds for final states of the type $B^0 \rightarrow P^0 Q^0$ [3], where P^0 and Q^0 represent any CP eigenstate spin-0 neutral particles (e.g. $P^0 = K_S^0$ and $Q^0 = \pi^0$). The effect of strong interaction is estimated to possibly be as large as 0.1 [4, 5]. Any significant deviation from this expectation would be a manifestation of new physics.

Since the S value for the non-resonant contribution is not expected to change significantly as a function of $K_S^0 \pi^0$ invariant mass ($M_{K_S^0 \pi^0}$) [5], from experimental viewpoint, we perform two measurements: one for $B^0 \rightarrow K^0 (\pi^+ K_S^0 \pi^-)$ by requiring $M_{K_S^0 \pi^0}$ to lie in the range $0.8 \text{ GeV} = c^2 < M_{K_S^0 \pi^0} < 1.0 \text{ GeV} = c^2$ and the other for the full range of $M_{K_S^0 \pi^0}$ below $1.8 \text{ GeV} = c^2$. For simplicity, we refer these two analyses as K^0 and $K_S^0 \pi^0$, respectively. The measurement for K^0 is theoretically cleaner than the measurement for $K_S^0 \pi^0$, on the other hand, $K_S^0 \pi^0$ has more statistical power than K^0 . Similar measurements have also been previously reported by Belle [6], and BaBar [7]. In this paper, we update the measurements of CP parameters for $B^0 \rightarrow K^0$ and $B^0 \rightarrow K_S^0 \pi^0$ based on a data sample that contains 535×10^6 $B\bar{B}$ pairs.

At the KEKB energy-asymmetric e^+e^- (3.5 on 8.0 GeV) collider [8], the (4S) is produced with a Lorentz boost of $\beta = 0.425$ along the z axis, which is defined as the direction antiparallel to the e^+ beam direction. In the decay chain $(4S) \rightarrow B^0 \bar{B}^0 \rightarrow f_{\text{sig}} f_{\text{tag}}$, where one of the B mesons decays at time t_{sig} to a final state f_{sig} , which is our signal mode, and the other decays at time t_{tag} to a final state f_{tag} that distinguishes between B^0 and \bar{B}^0 , the decay rate has a time dependence given by

$$P(t) = \frac{e^{-t/\tau_{B^0}}}{4\tau_{B^0}} [1 + qS \sin(m_d t) + A \cos(m_d t)] \quad (1)$$

Here S and A are CP-violation parameters, τ_{B^0} is the B^0 lifetime, m_d is the mass difference between the two B^0 mass eigenstates, t is the time difference $t_{\text{sig}} - t_{\text{tag}}$, and the b-flavor charge $q = +1$ (-1) when the tagging B meson is a B^0 (\bar{B}^0). Since the B^0 and \bar{B}^0 mesons are approximately at rest in the (4S) center-of-mass system (c.m.s.), t can be determined from the displacement in z between the f_{sig} and f_{tag} decay vertices: $t' = (z_{\text{sig}} - z_{\text{tag}})/c = \beta \gamma t = \beta \gamma (z_{\text{sig}} - z_{\text{tag}})/c$.

The Belle detector is a large-solid-angle magnetic spectrometer that consists of a silicon vertex detector (SVD), a 50-layer central drift chamber (CDC), an array of aerogel threshold Cerenkov counters (ACC), a barrel-like arrangement of time-of-flight scintillation counters (TOF), and an electromagnetic calorimeter comprised of CsI(Tl) crystals (ECL) located inside a superconducting solenoid coil that provides a 1.5 T magnetic field. An iron flux-return located outside of the coil is instrumented to detect K_L^0 mesons and to identify muons (KLM). The detector is described in detail elsewhere [9]. Two inner detector configurations were used. A 2.0 cm beam pipe and a three layer silicon vertex detector (SVD1) were used for the first sample of 152×10^6 $B\bar{B}$ pairs, while a 1.5 cm beam pipe, a four layer silicon

detector (SVD 2) and a small-cell inner drift chamber were used to record the remaining $383 \cdot 10^6$ $B\bar{B}$ pairs [10].

For high energy prompt photons, we select an isolated cluster in the ECL that has no corresponding charged track, and has the largest energy in the center-of-mass system (c.m.s.). We require $1.4 \text{ GeV} < E^{\text{c.m.s.}} < 3.4 \text{ GeV}$. For the selected photon, we also require $E_9 = E_{25} > 0.95$, where $E_9 = E_{25}$ is the ratio of energies summed in $3 \cdot 3$ and $5 \cdot 5$ arrays of CsI(Tl) crystals around the center of the shower. In order to reduce the background from π^0 or η , photons for candidate $\pi^0 \rightarrow \gamma\gamma$ or $\eta \rightarrow \gamma\gamma$ decays are not used; we reject photon pairs that satisfy $L_{\pi^0} < 0.18$ or $L_{\eta} < 0.18$, where $L_{\pi^0(\eta)}$ is a $\pi^0(\eta)$ likelihood described in detail elsewhere [11]. The polar angle of the photon direction in the laboratory frame is restricted to the barrel region of the ECL ($33^\circ < \theta < 128^\circ$) for SVD 1 data, but is extended to the end-cap regions ($17^\circ < \theta < 150^\circ$) for SVD 2 data due to the reduced material in front of the ECL.

Neutral kaons (K_S^0) are reconstructed from two oppositely charged pions that have the invariant mass within $6 \text{ MeV} = c^2$ (2%) of the K_S^0 nominal mass [16]. The $\pi^+\pi^-$ vertex is required to be displaced from the interaction point (IP) by a minimum transverse distance of 0.22 cm for high momentum ($> 1.5 \text{ GeV} = c$) candidates and 0.08 cm for those with momentum less than $1.5 \text{ GeV} = c$, and the direction of the pion pair momentum must agree with the direction defined by the IP and the two pion vertex point within 0.03 rad for high-momentum candidates, and within 0.1 rad for the remaining candidates. Neutral pions (π^0) are formed from two photons with the invariant mass within $16 \text{ MeV} = c^2$ (3%) of the π^0 mass. The photon momenta are then recalculated with a π^0 mass constraint. We then require the momentum of π^0 candidates in the c.m.s. to be greater than $0.3 \text{ GeV} = c$. The $K_S^0 \rightarrow \pi^0\pi^0$ invariant mass, $M_{K_S^0 \pi^0}$, is required to be less than $1.8 \text{ GeV} = c^2$.

We also reconstruct $B^0 \rightarrow K^+\pi^-$ and $B^+ \rightarrow K_S^0\pi^+$ candidates as control samples in a similar way. Charged pion tracks from $B^+ \rightarrow K_S^0\pi^+$ are required to originate from the IP (within 5 cm in z and 1.4 cm in r) and that the transverse momentum (p_t) is greater than $0.1 \text{ GeV} = c$. We also require that the π^+ candidate cannot be identified as any other particle species (K^+ ; p^+ ; e^+ and μ^+). Charged pions and kaons in the $B^0 \rightarrow K^+\pi^-$ control sample are required to satisfy the same IP and p_t requirements described above. Charged tracks not identified as K^+ candidates are assumed to be pions.

The $B^0 \rightarrow K_S^0\pi^0$ and $B^+ \rightarrow K_S^0\pi^+$ modes are reconstructed simultaneously and a single candidate is selected from possible multiple candidates amongst the two modes in order to reduce the cross-feed background from $B^+ \rightarrow K_S^0\pi^+$ in $B^0 \rightarrow K_S^0\pi^0$. The best candidate selection is based on the event likelihood ratio $LR(F)$ that is obtained from a Fisher discriminant F [12], which uses the extended modified Fox-Wolfgram moments [13] as discriminating variables. We select a candidate that has the largest $LR(F)$. We form two kinematic variables: the energy difference $E_{\pi^0} = E_B^{\text{c.m.s.}} - E_{\text{beam}}^{\text{c.m.s.}}$ and the beam-energy constrained mass $M_{bc} = \frac{(E_{\text{beam}}^{\text{c.m.s.}})^2 - (p_B^{\text{c.m.s.}})^2}{2E_{\text{beam}}^{\text{c.m.s.}}}$, where $E_{\text{beam}}^{\text{c.m.s.}}$ is the beam energy, $E_B^{\text{c.m.s.}}$ and $p_B^{\text{c.m.s.}}$ are the energy and the momentum of the candidate in the c.m.s. The t region of $E - M_{bc}$ to extract signal fraction is $0.3 \text{ GeV} < E < 0.5 \text{ GeV}$ and $5.2 \text{ GeV} = c^2 < M_{bc}$. The signal region, events within which are used in the CP test, is defined as $0.2 \text{ GeV} < E < 0.1 \text{ GeV}$ and $5.27 \text{ GeV} = c^2 < M_{bc} < 5.29 \text{ GeV} = c^2$.

In order to suppress the background contribution from continuum light quark pair production processes ($e^+e^- \rightarrow qq$ with $q = u; d; s; c$), which we refer to as qq hereafter, we form another likelihood ratio $LR(F, \cos \theta_B, \cos \theta_H)$ by combining F with $\cos \theta_B$ and $\cos \theta_H$, where θ_B is the polar angle of the B meson candidate momentum in the laboratory frame and θ_H

is the helicity angle defined as the kaon momentum direction in the K^- rest frame. The helicity distribution for signal is obtained from the $B^0 \rightarrow K^+ K^-$ sample for three mass regions: $0.8 \text{ GeV} = c^2 < M_{K_S^0} < 1.0 \text{ GeV} = c^2$ (MR1), $1.3 \text{ GeV} = c^2 < M_{K_S^0} < 1.55 \text{ GeV} = c^2$ (MR2), and the remaining range up to $1.8 \text{ GeV} = c^2$ (MR3). The background helicity distribution is determined in a similar way; in addition, a helicity dependent efficiency correction is applied. Specific LR ($F, \cos \theta_B, \cos \theta_H$) selection criteria are applied depending on both the mass region and the flavor tagging information.

The b-flavor of the accompanying B meson is identified from inclusive properties of particles that are not associated with the reconstructed signal decay. The algorithm for flavor tagging is described in detail elsewhere [14]. We use two parameters, q defined in Eq. (1) and r , to represent the tagging information. The parameter r is an event-by-event flavor-tagging dilution factor that ranges from 0 to 1; $r = 0$ when there is no flavor discrimination and $r = 1$ implies unambiguous flavor assignment. It is determined by using MC and is only used to sort data into seven r intervals. We set the wrong tag fraction to 0.5 if r is less than or equal to 0.1. Events with $r > 0.1$ are sorted into six r intervals. The wrong tag fraction w and the difference $w - \bar{w}$ between the B^0 and \bar{B}^0 decays are determined for each of the six r intervals from data.

The vertex position of the signal-side decay of $B^0 \rightarrow K_S^0 K^0$ and $B^+ \rightarrow K_S^0 K^+$ is reconstructed from the K_S^0 trajectory with a constraint on the IP; the IP profile ($x' = 100 \text{ m}, y' = 5 \text{ m}$) is convolved with the finite B flight length in the plane perpendicular to the z axis. The K_S^0 vertex is displaced from the B vertex and often lies outside of the SVD. When the K_S^0 vertex can be reconstructed inside the SVD, the time-dependent CP asymmetry can be measured. Both pions from the K_S^0 decay are required to have enough hits in the SVD in order to reconstruct the K_S^0 trajectory with high resolution; at least one layer with hits on both sides and at least one additional hit in the z side of the other layers for SVD 1, and at least two layers with hits on both sides for SVD 2. The other (tag-side) B vertex is determined from well reconstructed tracks that are not assigned to the signal side [18]. A constraint to the IP profile is also imposed.

After all the selections are applied, we obtain 4078 candidates in the $E - M_{bc}$ region, of which 406 are in the signal box. We perform an unbinned maximum likelihood (UML) fit to the $E - M_{bc}$ distribution in order to resolve signal, $B\bar{B}$ background and qq background components. The signal probability density function (PDF) is obtained from MC. We use a two-dimensional histogram of MC data, for which the peak position and the width are corrected using the $B^0 \rightarrow K^+ K^-$ control sample. The two dimensional PDF for $B\bar{B}$ background is obtained from MC. For qq background, we use the product of two one-dimensional PDFs: the ARGUS parameterization [15] for M_{bc} and a second order polynomial for E . Five parameters, which are the signal fraction, the rare B background fraction, ARGUS shape parameter α , and two coefficients of polynomial, are the free parameters in the fit.

We first fit the entire $M_{K_S^0}$ region, and then fit the MR1, MR2 and MR3 mass regions separately with the three background shape parameters fixed at the values obtained from the fit to the full range. Figure 1 shows $E - (M_{bc})$ projection of the fit result in the $M_{bc} - (E)$ signal slice for the entire $M_{K_S^0}$ region. We find $112.5 \pm 12.0, 28.7 \pm 7.1, 35.2 \pm 10.0$ signal events, and $7.7 \pm 4.2, 4.1 \pm 2.4, 5.3 \pm 5.2$ $B\bar{B}$ background events in MR1, MR2, MR3, respectively. The signal to noise ratios are 1.91, 0.81, and 0.35, respectively. As expected, in the K^0 mass region the S/N ratio is high.

We determine S and A from an UML fit to the observed fit distribution. The PDF expected for the signal distribution, $P_{sig}(t; S; A; q; w; \bar{w})$, is given by the time dependent

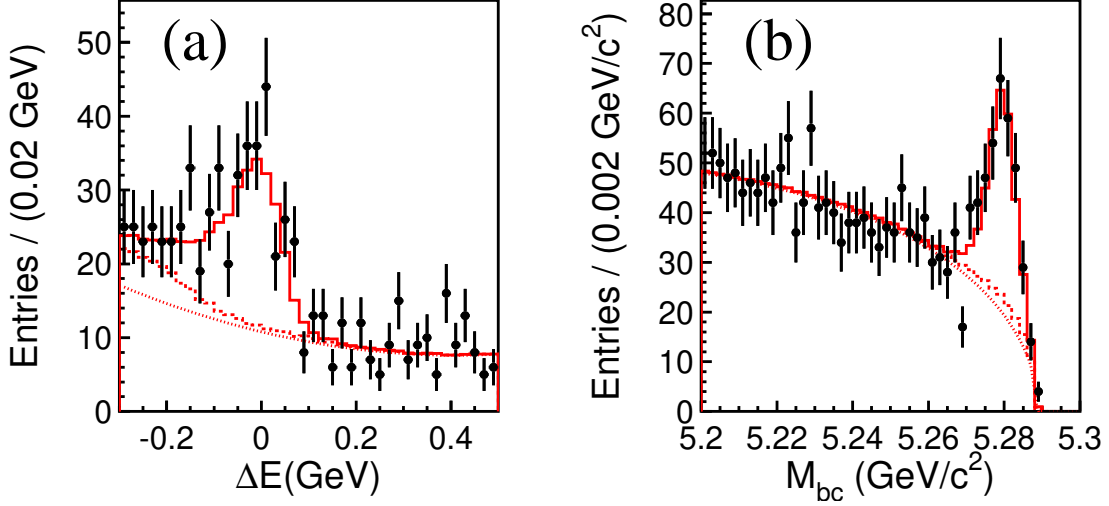


FIG. 1: (a) E distribution within the M_{bc} signal region and (b) M_{bc} distribution within the E signal region for the whole $M_{K_S^0}$ region. Points with error bars are measured data. The solid curves show the t results. The dotted curves show the qq background contributions while the dashed curves show the sum of qq and $B\bar{B}$ background contributions.

decay rate [Eq. (1)] with fixed τ_{B^0} and m_d at their world-average values [16], which is modified to incorporate the effect of incorrect flavor assignment. The distribution is convolved with the proper-time interval resolution function R_{sig} , which takes into account the finite vertex resolution. The parameterization of R_{sig} is the same as that used for the $B^0 \rightarrow K_S^0 \pi^0$ decay [17]. R_{sig} is first derived from flavor-specific B decays [18] and modified by additional parameters that rescale vertex errors to account for the fact that there is no track directly originating from the B meson decay point.

The PDF for $B\bar{B}$ background events ($P_{B\bar{B}}$) is modeled in the same way as signal, but with different lifetime parameter and CP parameters, while the resolution function $R_{B\bar{B}}$ is the same as R_{sig} . The effective lifetime of $B\bar{B}$ background is obtained from a fit to MC sample, which gives 1.356 ± 0.045 ps. The background is assumed to have no CP asymmetry; possible deviations from this assumption ($S = 0.2$ and $A = 0.2$) are taken into account in the systematic error.

The PDF for qq background events, P_{qq} , is modeled as a sum of exponential and prompt components, and is convolved with a double Gaussian which represents the resolution function R_{qq} for the background. All parameters in P_{qq} and R_{qq} are determined by a fit to the t distribution of a background-enhanced sample in the E - M_{bc} sideband region.

For each event, the following likelihood function is evaluated:

$$\begin{aligned}
 P_i = & (1 - f_{o1}) \prod_{j=1}^{Z+1} \left[f_{sig} P_{sig}(t_j^0) R_{sig}(t_i - t_j^0) \right. \\
 & + f_{B\bar{B}} P_{B\bar{B}}(t_j^0) R_{B\bar{B}}(t_i - t_j^0) \\
 & + (1 - f_{sig} - f_{B\bar{B}}) P_{qq}(t_j^0) R_{qq}(t_i - t_j^0) \left. d(t_j^0) \right] \\
 & + f_{o1} P_{o1}(t_i);
 \end{aligned} \tag{2}$$

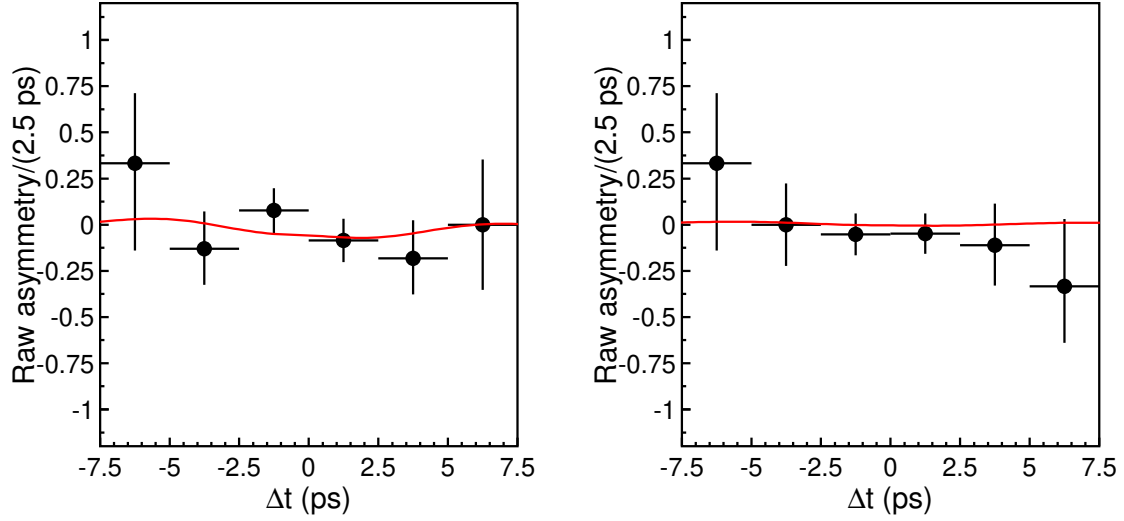


FIG. 2: Asymmetry in each Δt bin for $B^0 \rightarrow K_S^0$ with $0 < r \leq 0.5$ (left) and $0.5 < r \leq 1.0$ (right).

Solid curves show the results of the UML fits.

where P_{ol} is a Gaussian function that represents a small outlier component with fraction f_{ol} [18]. The signal and background probability are calculated on an event by event basis using the results of the two-dimensional $E-M_{bc}$ fit and then multiplying by a factor that depends on the flavor tagging bin r . The r distributions of signal and qq background events are estimated by repeating the $E-M_{bc}$ fit procedure for each r interval. The $B\bar{B}$ background distribution is estimated from MC since the number of $B\bar{B}$ background events in data is limited.

The only free parameters in the final CP fit to $B^0 \rightarrow K_S^0$ are $S_{K_S^0}$ and $A_{K_S^0}$, which are determined by maximizing the likelihood function $L = \prod_i P_i(t_i; S; A)$ where the product is over all events. We obtain

$$\begin{aligned} S_{K_S^0} &= 0.10 \pm 0.31(\text{stat}) \pm 0.07(\text{syst}); \\ A_{K_S^0} &= 0.20 \pm 0.20(\text{stat}) \pm 0.06(\text{syst}); \end{aligned}$$

We define the raw asymmetry in each Δt bin by $(N_{q=+1} - N_{q=-1}) / (N_{q=+1} + N_{q=-1})$, where $N_{q=+1(-1)}$ is the number of observed candidates with $q = +1(-1)$. Figure 2 shows the raw asymmetries for the K_S^0 events. Note that these are simple projections onto the Δt axis, and do not reflect other event-by-event information (such as the signal fraction, the wrong tag fraction and the vertex resolution), which is used in the UML fit for S and A . The likelihood contour in S and A plane is shown in Fig 3. Each of S and A is consistent with zero within one standard deviation. We perform the following fits to confirm the validity of the result: a B^+ lifetime fit for the $B^+ \rightarrow K_S^+$ sample gives 1.49 ± 0.10 ps, which is consistent with nominal B^+ lifetime [16]; a B^0 lifetime fit for the $B^0 \rightarrow K_S^0$ sample gives $1.53^{+0.19}_{-0.17}$ ps, which is consistent with nominal B^0 lifetime [16]; and a CP asymmetry fit for the $B^+ \rightarrow K_S^+$ sample gives an asymmetry consistent with zero ($S = 0.20 \pm 0.18$, $A = 0.05 \pm 0.11$). This is expected since the charged decay is completely flavor specific

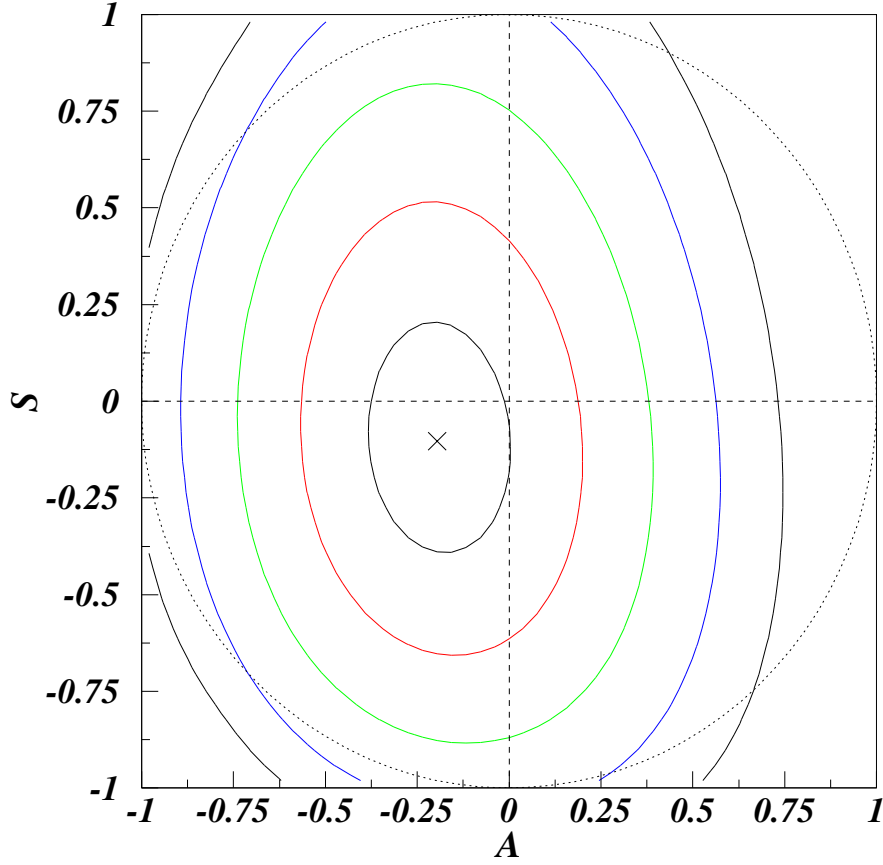


FIG. 3: Contour plot of likelihood. Cross is the best fit point, 5 lines around the cross are 1, 2, 3, 4, and 5 deviated lines. Dotted circle is the physical boundary. Systematic errors not included.

regardless of the photon polarization. A fit to MR1 data gives

$$S_{K^0} = 0.32^{+0.36}_{-0.33} \text{ (stat)} \quad 0.05 \text{ (syst)};$$

$$A_{K^0} = 0.20 \quad 0.24 \text{ (stat)} \quad 0.05 \text{ (syst)};$$

A fit to non-MR1 data gives $S = +0.50 \quad 0.61$ and $A = 0.20 \quad 0.37$. These results are consistent with those from the full $M_{K_S^0}$ sample.

We evaluate systematic uncertainties in the following categories by fitting the data with each fixed parameter shifted by its error: uncertainties from physics parameters such as m_{B^0} , effective lifetime and CP asymmetry of $B\bar{B}$ background, uncertainties in the knowledge of $q\bar{q}$ background fit PDF and the resolution function, uncertainties in the flavor tagging, uncertainties in the signal and $B\bar{B}$ background fractions, uncertainties in the signal and $B\bar{B}$ resolution functions. A possible bias in the fit is checked by fitting a large MC sample. The fit result is consistent with the input value within the statistical error. We quote the statistical error as the possible fit bias. Uncertainty due to the vertex reconstruction is estimated by using the $B^0 \rightarrow J/\psi K_S^0$ control sample, where the tracks from J/ψ are ignored for the study of the signal side vertex reconstruction using the K_S^0 trajectory. The effect of SVD

category	$K_S^0 \rightarrow 0$		K^0	
	S	A	S	A
physics	0.009	0.012	0.008	0.009
background t	0.007	0.004	0.003	0.002
flavor tagging	0.007	0.005	0.010	0.005
signal fraction	0.061	0.033	0.028	0.009
t bias	0.006	0.004	0.006	0.004
resolution function	0.025	0.010	0.037	0.009
vertex reconstruction	0.009	0.021	0.009	0.021
tag-side interference	0.002	0.041	0.002	0.041
sum	0.068	0.059	0.050	0.049

TABLE I: Systematic Errors

misalignment is estimated by artificially displacing the SVD sensors in a random manner; the standard deviation of these shifts and rotations are 15 μm and 0.15m rad, respectively. Effects of tag-side interference [19] are estimated using $B^0 \rightarrow D^+ \pi^-$. All these contributions to the systematic errors are given in Table I and are summed in quadrature to give 0.07 (0.05) for S and 0.06 (0.05) for A for $B^0 \rightarrow K_S^0 \pi^0$ ($B^0 \rightarrow K^0 \pi^0$).

Ensemble tests are carried out with MC pseudo-experiments using S and A obtained by the fit as the input parameters. From 10,000 pseudo-experiments, we find that the statistical errors obtained in our measurement are within expectations.

In summary, we have performed a measurement of the time-dependent CP asymmetry in the decay $B^0 \rightarrow K_S^0 \pi^0$ with $K_S^0 \pi^0$ invariant mass up to $1.8\text{GeV} = c^2$, based on a sample of 535×10^6 $B\bar{B}$ pairs. We obtain CP-violation parameters $S_{K_S^0 \pi^0} = 0.10 \pm 0.31(\text{stat}) \pm 0.07(\text{syst})$ and $A_{K_S^0 \pi^0} = 0.20 \pm 0.20(\text{stat}) \pm 0.06(\text{syst})$ for the full $K_S^0 \pi^0$ invariant mass region, and $S_{K^0 \pi^0} = 0.32^{+0.36}_{-0.33}(\text{stat}) \pm 0.05(\text{syst})$ and $A_{K^0 \pi^0} = 0.20 \pm 0.24(\text{stat}) \pm 0.05(\text{syst})$ for the mass region around K^0 (892). This measurement supersedes our previous measurement [6]. We do not find any significant CP asymmetry, and therefore no indication of new physics from right handed currents, with the present statistics.

We thank the KEKB group for the excellent operation of the accelerator, the KEK cryogenics group for the efficient operation of the solenoid, and the KEK computer group and the National Institute of Informatics for valuable computing and Super-SINET network support. We acknowledge support from the Ministry of Education, Culture, Sports, Science, and Technology of Japan and the Japan Society for the Promotion of Science; the Australian Research Council and the Australian Department of Education, Science and Training; the National Science Foundation of China and the Knowledge Innovation Program of the Chinese Academy of Sciences under contract No. 10575109 and IHEP-U-503; the Department of Science and Technology of India; the BK21 program of the Ministry of Education of Korea, and the CHEP SRC program and Basic Research program (grant No. R01-2005-000-10089-0) of the Korea Science and Engineering Foundation; the Polish State Committee for Scientific Research under contract No. 2P03B 01324; the Ministry of Science and Technology of the Russian Federation; the Slovenian Research Agency; the Swiss National Science Foundation; the National Science Council and the Ministry of Education of Taiwan; and the

- [1] D. Atwood, M. Gronau and A. Soni, *Phys. Rev. Lett.* 79, 185 (1997).
- [2] M. Matsumori and A. I. Sanda, *Phys. Rev. D* 73, 114022 (2006).
- [3] D. Atwood, T. Gershon, M. Hazumi and A. Soni, *Phys. Rev. D* 71, 076003 (2005).
- [4] B. Grinstein, Y. Grossman, Z. Ligeti and D. Pirjol, *Phys. Rev. D* 71, 011504 (2005).
- [5] B. Grinstein and D. Pirjol, *Phys. Rev. D* 73, 014013 (2006).
- [6] Y. Ushiroda et al., *Phys. Rev. Lett.* 94, 231601 (2005).
- [7] BaBar Collaboration, B. Aubert et al., *Phys. Rev. D* 72, 051103 (2005).
- [8] S. Kurokawa and E. Kikutani, *Nucl. Instr. and Meth. A* 499, 1 (2003).
- [9] Belle Collaboration, A. Abashian et al., *Nucl. Instr. and Meth. A* 479, 117 (2002).
- [10] Y. Ushiroda (Belle SVD2 Group), *Nucl. Instr. and Meth. A* 511, 6 (2003).
- [11] Belle Collaboration, P. Koppenburg et al., *Phys. Rev. Lett.* 93, 061803 (2004).
- [12] R. A. Fisher, *Annals Eugen.* 7, 179 (1936).
- [13] Belle Collaboration, K. Abe et al., *Phys. Rev. Lett.* 91, 261801 (2003).
- [14] H. Kakuno, K. Hara et al., *Nucl. Instr. and Meth. A* 533, 516 (2004).
- [15] ARGUS Collaboration, H. Albrecht et al., *Phys. Lett. B* 241, 278 (1990).
- [16] W. M. Yao et al. (Particle Data Group), *Journal of Physics G* 33, 1 (2006).
- [17] Belle Collaboration, K. F. Chen et al., *Phys. Rev. D* 72, 12004 (2005).
- [18] Belle Collaboration, K. Abe et al., *Phys. Rev. D* 71, 072003 (2005) ; H. Tajima et al., *Nucl. Instr. and Meth. A* 533, 370 (2004).
- [19] O. Long, M. Baak, R. N. Cahn and D. Kirkby, *Phys. Rev. D* 68, 034010 (2003).